Materials Science-Poland, Vol. 25, No. 2, 2007

Magnetic properties of cementite (Fe_3C) nanoparticle agglomerates in a carbon matrix

K. LIPERT[1*], J. KAŹMIERCZAK[1], I. PEŁECH[2], U. NARKIEWICZ[2], A. ŚLAWSKA-WANIEWSKA[1], H.K. LACHOWICZ[1]

[1]Institute of Physics, Polish Academy of Sciences, Al. Lotników 32/46, 02-668, Warsaw

[2]Institute of Chemical and Environment Engineering, Technical University of Szczecin, al. Piastów 19, 70-322 Szczecin

Magnetic properties of two FeC samples with different amounts of carbon have been studied. In both cases, the amount of carbon was well above the mass sufficient to transform nanocrystalline iron into iron carbide (cementite). Through the dc magnetic and transmission electron microscopy (TEM) measurements it was shown that cementite nanoparticles formed agglomerates; the size distribution of these nanoparticles was very wide, and superparamagnetic-like behaviour was not observed even at room temperature.

Key words: *superparamagnetism; coercivity; iron carbide; Stoner–Wohlfarth model*

1. Introduction

First theoretical considerations and calculations of the critical size of magnetic particle (typically few nanometers), that is the size below which the most energetically favourable magnetic state is a single domain state, were carried out by Charles Kittel in 1946 [1]. Superparamagnetism is the phenomenon by which the system containing single domain magnetic nanoparticles, dispersed in a nonmagnetic matrix, may exhibit at temperatures above the so-called blocking temperature T_B, a behaviour similar to that of a paramagnetic material. At a temperature higher than the blocking temperature, a stable bulk magnetization cannot be established because of thermal fluctuations acting on each particle in a system, and so the bulk material exhibits superparamagnetism (SPM). At temperatures below T_B, thermal fluctuations cannot overcome the energy barrier connected with the magneto-crystalline anisotropy en-

*Corresponding author, e-mail: lipert@ifpan.edu.pl

ergy, and then magnetic moments of particles are confined in random directions, lying along easy axis of magnetization and cannot change their directions spontaneously from one easy direction to the other. The first model of monodispersed, non-interacting, single domain magnetic particles with uniaxial anisotropy, embedded in a nonmagnetic matrix was proposed by Stoner and Wolhfarth [2].

The thermal relaxation of magnetic nanoparticles is excellently described by the Arrhenius–Néel formula [3]:

$$t_{\mathrm{rel}} = t_0 \exp\left(\frac{E_A}{k_B T}\right) \tag{1}$$

where t_{rel} is the relaxation time of the particle magnetic moment, E_A is the anisotropy energy barrier, t_0 is the characteristic relaxation time, ranging typically from 10^{-11} to 10^{-9} s. In the absence of external magnetic field, the anisotropy barrier E_A is proportional to the particle volume, V, and can be expressed as $E_A = KV\sin^2\alpha$, where K is the effective magnetic anisotropy constant and α is the angle between magnetic moment of the particle and its easy magnetization direction.

In the recent decade, great attention has been focused on magnetic nanoparticles [4, 5] because of their unique physical properties and also because of the possibility of their practical application in medicine and biotechnology (e.g., hyperthermia [6], targeted drug delivery [7], contrast agents in MRI [8]) as well as in catalysis, magnetic separation, gas sensors and many others. The aim of the present work was to investigate structural characteristics and magnetic properties of nanoparticle agglomerates of iron carbide (Fe_3C) embedded in a carbon matrix.

2. Preparation of samples and shape characterization

Samples were prepared in the process of carburisation of nanocrystalline iron with ethylene [9]. The nanocrystalline iron was doped with a small amount of two promoter oxides (Al_2O_3 and CaO). The samples were obtained by the fusion of magnetite with the promoter oxides. The alloy obtained was crushed after cooling and then sieved to separate the fraction of 1.2–1.5 mm. To obtain metallic iron, polythermal reduction with hydrogen was used. The pyrophoric specimens obtained after reduction were passivated using nitrogen with a 0.5% addition of oxygen. The chemical composition after passivation was determined using inductively coupled plasma atomic emission spectroscopy (AES-ICP). Besides iron, the samples contained 2.9 wt. % of Al_2O_3, 3.0 wt. % of CaO, 0.3 wt. % of SiO_2, and 1 wt. % of other metal oxides (Mg, Ni, Cr, Ti, V).

The carburisation process was carried out in a spring thermobalance. A single layer of grains of the sample was placed in a platinum basket and hung in the thermobalance. Changes in the mass of samples were recorded with a cathetometer. Before carburisation, the samples were reduced under hydrogen at a temperature rising from

293 to 773 K. After reduction (when a constant mass of the sample was reached), the carburisation process was started using ethylene (40 dm^3/h). The carburisation was

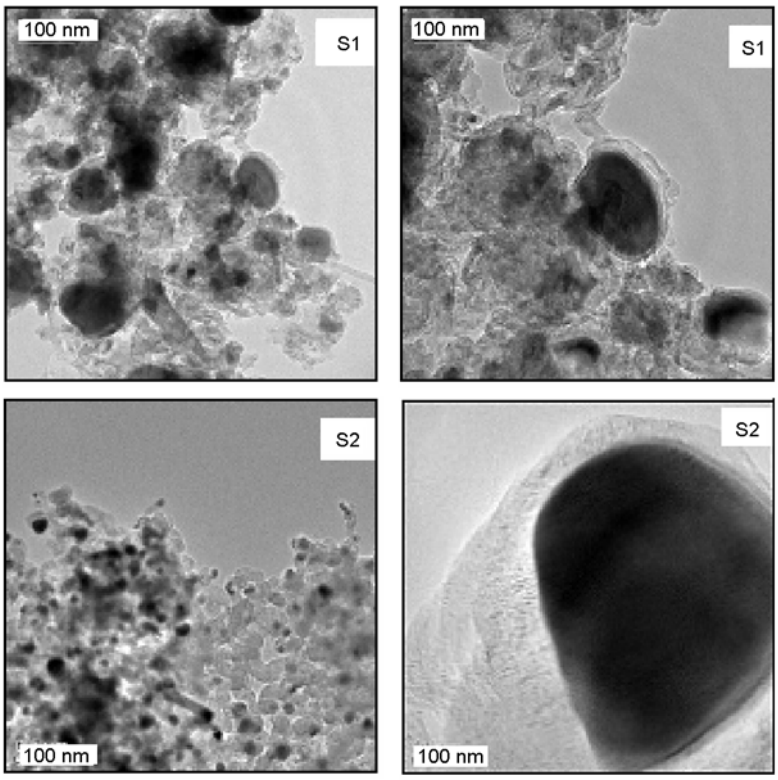

Fig. 1. Transmission electron microscope (TEM) pictures
with various enlargements for samples 1 (upper) and 2 (bottom)

carried out isothermally, at the temperature of 773 K. The products of the carburisation of nanocrystalline iron with ethylene are iron carbide and carbon deposits. Iron carbide is formed only as cementite, which crystallizes in an orthorhombic structure. Its particles form relatively large agglomerates (see Fig. 1, left). Individual particles are also large (right). Such a shape of nanoparticles has large impact on magnetic properties of the samples, as will be shown in Sec. 3.

3. Measurements of magnetic parameters

Magnetic parameters were measured using vibrating sample magnetometer VSM. Thermo-remanence magnetization (not shown here), hysteresis loops, zero field- and field-cooled measurements (M_{ZFC} and M_{FC}) were carried out in the temperature range from 5 to 300 K. Figure 2 shows the hysteresis loops for both samples at 5 K and 300 K. It is clear that both samples did not exhibit superparamagnetic-like behaviour

within this temperature range, since even at room temperature their coercivity is far from zero.

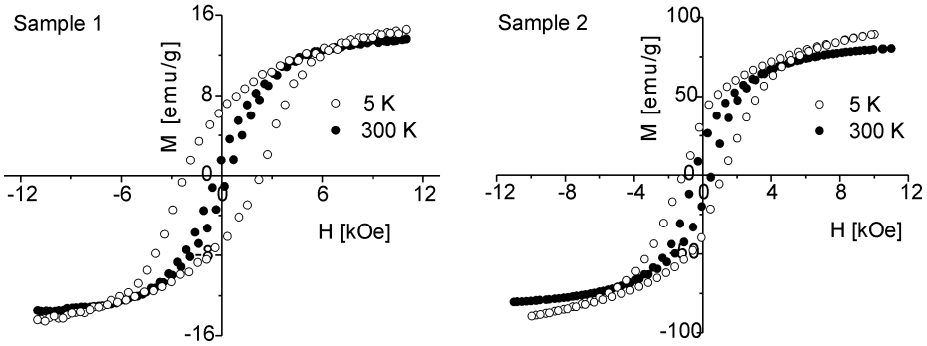

Fig. 2. Hysteresis loops at 5 K and 300 K for samples 1 and 2

Figure 3 shows the so called zero field- (ZFC) and field-cooled (FC) magnetization curves recorded in the presence of external magnetic field of 100 Gs. Using the dependences presented in Fig. 3, one can find the distribution of the blocking temperature in the studied system. As shown in [10], the derivative of the difference of these two magnetizations by temperature $d(M_{ZFC} - M_{FC})/dT$, represents the number of particles whose blocking temperature falls into the range of a given temperature. The calculated temperature dependence of the described relationship is shown in Fig. 3 for sample 1. As can be seen, the distribution of the blocking temperatures is very wide, showing, similarly as the hysteresis loops, that even at room temperature not all particles are superparamagnetic.

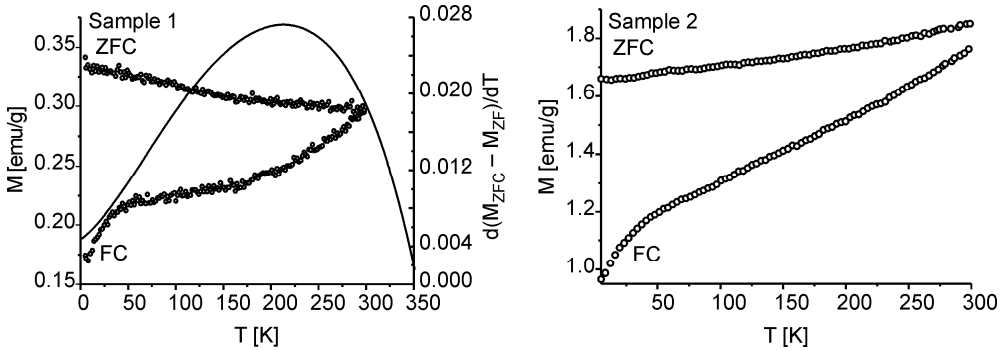

Fig. 3. Zero field- (ZFC) and field-cooled (FC) curves recorded at the field of 100 Gs for the samples S1 and S2; corresponding distribution of blocking temperatures for the sample S1 is also shown

At low temperature, where all the magnetic moments of a system of randomly oriented and non-interacting particles are blocked, the coercivity is equal to the value for monodomains, H_{C0}. At a sufficiently high temperature, when all moments fluctuate with

the relaxation time shorter than the measuring time, coercivity equals zero. For intermediate temperatures, the coercivity H_C can be evaluated from the formula [11]:

$$H_C(T) = H_{C0}\left[1-\left(\frac{T}{T_B}\right)^{1/2}\right] \tag{2}$$

where H_{C0} is the coercivity at $T = 0$ K and T_B is the blocking temperature of the largest particle in the system.

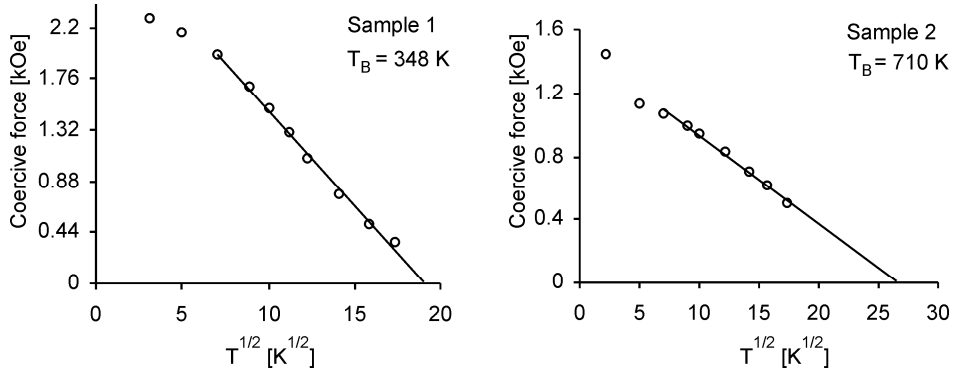

Fig. 4. Coercivity vs. square root temperature for the samples S1 and S2

Figure 4 shows the coercivity derived from the hysteresis loops measured for both samples, plotted as a function of the square root of temperature. As can be seen, both dependences are linear in the range of higher temperatures. The extrapolated values of the maximum blocking temperature T_B (i.e., blocking temperature of the largest particles) calculated according to the above equation are equal to 348 K and 710 K for the samples S1 and S2, respectively. It is worth to note, that the value of the remanence magnetization at low temperatures is very close to half of the value of saturation magnetization, being equal to 0.46 and 0.41 for the S1 and S2 sample, respectively. This seems to be in a good agreement with the Stoner–Wohlfarth model.

Table 1. Summary of certain properties of studied samples

Sample	Carbon mass increase m_C/m_{Fe}	Mass ratio m_{Fe_3C}/m_C	Coercive force* [kOe]	M_{REM}/M_{SAT}	T_B [K]
S1	1.687	0.662	0.365	0.46	348
S2	0.715	1.659	0.504	0.41	710

*At room temperature.

4. Conclusions

As can be seen in the TEM pictures, the particles form agglomerates which can behave like a large single particle because of the exchange interactions acting between particles forming individual agglomerates. The investigated particles display relatively wide distribution of their sizes resulting, in accordance with Eq. (1), in a wide distribution of the blocking temperatures. Since size of the particles is relatively large, larger than the critical size, they may exhibit a multi-domain magnetic structures. Both the studied samples do not display superparamagnetic like behaviour even at room temperature. Similarly, their blocking temperatures are well above the room temperature.

References

[1] KITTEL C., Phys. Rev., 70 (1946), 965.
[2] STONER E.C., WOHLFARTH E.P., IEEE Trans. Magn., 27 (1991), 3475.
[3] NÉEL L., Compt Rend. (Paris), 228 (1949), 604.
[4] ŚLAWSKA-WANIEWSKA A., GUTOWSKI M., LACHOWICZ H.K., KULIK T., MATYJA H., Phys. Rev. B, 46 (1992), 14594.
[5] DIDUKH P., NEDELKO O., ŚLAWSKA-WANIEWSKA A., J. Magn. Magn. Mater., 242 (2002), 1077.
[6] YOSHIDA J., KOBAYASHI T., J. Magn. Magn. Mater., 194 (1999), 176.
[7] PANATAROTTO D., PRTIDOS C.D., HOEBEKE J., BROWN F., KRAMER E., BRIAND J.P., MULLER S., PRATO M., BIANCO A., Chem. Biol., 10 (2003), 961.
[8] WEISSLEDER R., ELIZONDO G., WITTENBURG J., RABITO C.A., BENGELE H.H., JOSEPHSON L., Radiol., 175 (1990), 489.
[9] NARKIEWICZ U., KUCHAREWICZ I., ARABCZYK W., LENART S., Mater. Sci.-Poland, 23 (2005), 939.
[10] JIN LU LU, HONG YUAN DENG, HUEI LI HUAN, J. Magn. Magn. Mater., 209 (2000), 37.
[11] CANDELA G.A., HAINES R.A., Appl. Phys. Lett., 34 (1979), 868.

Received 7 May 2006
Revised 1 September 2006